Universal features in the electrical conductivity of icosahedral Al-transition-metal quasicrystals

Enrique Maciá
GISC, Departamento de Física de Materiales, Facultad de Físicas, Universidad Complutense, E-28040 Madrid, Spain
(Received 24 June 2002; published 25 November 2002)

In this work we report the existence of certain universal features in the temperature dependence of the electrical conductivity of Al-transition-metal icosahedral quasicrystals, extending the results previously reported on the inverse Matthiessen rule [D. Mayou, C. Berger, F. Cyrot-Lackmann, T. Klein, and P. Lanco, Phys. Rev. Lett. **70**, 3915 (1993)]. We propose a tentative classification scheme providing a unified description of the electrical conductivity curves over a broad temperature range. We introduce a phenomenological model describing the electrical conductivity of icosahedral quasicrystals, deriving closed analytical expressions. We compare our analytical results with suitable experimental data and illustrate the use of the introduced phenomenological coefficient in order to extract information about the electronic structure of the samples from a fitting analysis of the experimental conductivity curves.

DOI: 10.1103/PhysRevB.66.174203 PACS number(s): 61.44.Br, 71.20.−b, 72.10.−d

I. INTRODUCTION

During the last decade it has been progressively realized that thermodynamically stable quasicrystalline alloys[1] occupy an odd position among the well-ordered condensed-matter phases. In fact, since quasicrystals (QC's) consist of metallic elements and they exhibit a well-defined Fermi edge,[2] one should expect that QC's would behave as metals. Nonetheless, most of their purported transport properties[3–9] resemble a more semiconductorlike than metallic character.[10–13] To complete the puzzle, QC's exhibit an ideal ohmic behavior over a broad voltage range,[14] and the possibility that they also obey Wiedemann-Franz's law has been theoretically suggested.[15] Consequently, neither the notion of metal nor that of semiconductors apply to QC's, clearly demanding the introduction of a more adequate concept to describe them. A proper understanding of QC's should be able to encompass their peculiar electronic structure and their unusual transport properties within a unifying conceptual scheme. To this end, the possible existence of general laws, allowing for a systematic classification of QC's according to their related transport coefficients, appears as a very promising starting point.

The electrical conductivity of samples belonging to different icosahedral families has been extensively studied.[16–41] Measured data comprise a broad range of stoichiometric compositions, covering different temperature ranges within the interval 0.1 K to 1000 K. In this way, several anomalous properties have been reported, supporting the presence of a series of qualitative universal features in the temperature dependence of the electrical conductivity $\sigma(T)$. Thus (i) their electrical conductivity takes unusually low values for an alloy made of good metals, (ii) $\sigma(T)$ steadily increases as the temperature increases up to the melting point, (iii) the $\sigma(T)$ curve is extremely sensitive to minor variations in the sample stoichiometry, and (iv) the electrical conductivity decreases when the structural order of the sample is improved by annealing. Strong evidence of a possible quantitative universal behavior of the electrical conductivity of *i*-QC's was reported by Mayou and co-workers.[42] They observed that the conductivity curves of different quasicrystalline samples are nearly parallel up to about 1000 K, so that one can write[42]

$$\sigma(T)=\sigma(0)+\Delta\sigma(T), \tag{1}$$

where $\sigma(0)$ measures the sample-dependent residual conductivity,[43] and $\Delta\sigma(T)$ is proposed to be an almost sample-independent general function. This remarkable behavior, referred to as an *inverse* Matthiessen rule,[42] has been also observed in quasicrystalline approximants,[44] and even in amorphous phases prior to their thermally driven transition to the QC phase.[45] These findings indicate that the inverse Matthiessen rule may be a quite general property of structurally complex alloy phases closely related to quasicrystalline compounds.

Attending to the overall variation of their $\sigma(T)$ curves, however, *i*-QC's can be separated into two broad categories.[46] In the first class we have the AlCuFe and AlPdMn families, which are characterized by the presence of *broad minima* at about 10–20 K and 80–150 K, respectively. In the second class we have the (relatively) less conductive AlCuRu and AlPdRe families, exhibiting a monotonous growth over the entire considered temperature range. The $\sigma(T)$ curves of samples belonging to the second class can be then properly fitted in terms of power law functions of the form $\Delta\sigma(T)\sim AT^n$ $(1/2\leqslant n\leqslant 3/2)$, over a broad temperature range.[30,31] On the contrary, the $\sigma(T)$ curve of samples belonging to the first class cannot be properly described in terms of monotonous functions, at least in the temperature region below the minimum position.[47] In addition, at very low temperatures, AlPdRe samples belonging to the second class exhibit negative curvatures which can be well fitted in terms of stretched exponential functions of the form $\Delta\sigma(T)\sim\sigma_0\exp[-(T_0/T)^m]$, with $m=1/2$ or $1/4$.[48] Therefore, it is not possible to describe the $\Delta\sigma(T)$ function by means of a common mathematical expression for all the considered QC's.

Then, the question arises concerning the possible existence of a suitable physical mechanism supporting the presumed universality of the $\Delta\sigma(T)$ function. In fact, the parallelism of the $\sigma(T)$ curves is difficult to understand in terms of a classical thermally activated mechanism, since the tem-

perature dependence of $\sigma(T)$ does not follow an exponential law of the form $\exp(-E/k_BT)$, where k_B is the Boltzmann constant. An $\exp(-AT^{-1/4})$ law, characteristic of variable range hopping mechanisms, neither applies at low temperatures.[48] The inadequacy of the $\exp(-E/k_BT)$ fitting implies the absence of a conventional semiconductinglike gap in QC's.[21] Additional evidence comes from the fact that, for the heavily doped semiconductors, the $\sigma(T)$ curve decreases at high enough temperatures when all the impurity levels have become ionized. No evidence of such a limiting threshold has been observed in QC's.[5] Nevertheless, a recent combined analysis of the magnetic susceptibility and electrical conductivity temperature dependencies in the temperature range 3.9 to 1200 K suggests that thermal activation of carriers, involving two different activation energy scales, may play a significant role in the electronic transport of AlCuFe samples at temperatures above the Debye one.[49] On the other hand, signatures of electron-electron and spin-orbit interactions, chemical disorder effects, or quasiperiodicity effects have been inferred from the temperature dependence of σ, although their relative role is still awaiting a precise experimental and theoretical clarification.[48] Consequently, one would expect that different fits to the experimental data may be more or less adequate depending on the temperature ranges considered, since the relative importance of different physical mechanisms at work will depend on their own temperature scales.

In the low-temperature regime ($0.5\ \mathrm{K} \lesssim T \lesssim 5\ \mathrm{K}$) the variation of $\sigma(T)$ has been shown to be in accordance with electron-electron interaction effects. At higher temperatures ($10\ \mathrm{K} \lesssim T \lesssim 30\ \mathrm{K}$) the $\sigma(T)$ behavior can be described in terms of weak localization effects. Therefore, the low-temperature and magnetic-field dependencies of the electrical conductivity in QC's have been usually analyzed in terms of quantum interference effects.[16,19,22,24,25,50] These theories were elaborated for metals in the weak disorder limit. Thus, it is intriguing how concepts originally developed to describe amorphous solids can be successful in describing long-range ordered systems such as QC's. It should be noted that, due to the number of degrees of freedom available, performing complete fits in the context of quantum interference theories is a difficult task. Authors often get large error bars for the microscopic parameters extracted, or consider different approaches which do not all give exactly the same results.[51] It may then be possible that quantum interference effects were indeed playing a role, but acting on significantly larger (20–30 Å) length scales than those typical of disordered metals (a few Å). In that case, the obtained fitting parameters will be referring to physical attributes of aggregates of atoms rather than to atomically sized defects.

Alternative approaches, aimed to exploit the physical implications of the quasiperiodic order notion, have also been considered. The theoretical prediction that critical electronic states decaying as a power law given by $\psi \propto r^{-\beta}$ should lead to a conductivity dependence of the form $\sigma \propto T^{2\beta/d}$, where d is the dimensionality of the system,[52–55] has been invoked to justify power-law fittings. Variable range hopping conduction between strongly localized states, related to a self-similar hierarchical nesting of atomic clusters,[56] or a multiple-valley fractional Fermi-surface model for the electronic structure of QC's[57–59] have been also considered to explain the anomalous transport properties. In that case, localization is caused by constructive interference of electronic states stemming from the characteristic symmetry of QC's, at variance with the Anderson localization arising from disorder.[60,61] These approaches have obtained partial success in describing different experimental data, thus highlighting the convenience for a suitable theory of quasicrystalline matter, able to treat different temperature scales within a coherent picture.

Keeping in mind these results it seems reasonable to assume that any adequate mathematical expression for the $\Delta\sigma(T)$ function in Eq. (1) should include several contributions, each one describing the physical mechanism mainly contributing at a given temperature. In this sense it becomes appealing to revisit the possible relationship between the electronic structure and transport properties in high-quality QC's. To this end, we shall exploit the dependence of the $\sigma(T)$ curve on the fitness between the energy scale of the different electronic spectral features and the thermal energy window width, $\sim k_BT$, around the Fermi level at a given temperature.[62–64] Following this path we have previously considered simplified models for the electronic density of states (DOS) of *i*-QC's, estimating the influence of their electronic structure on several transport coefficients.[65–67]

The main goal of the present work is to analyze the existence of universal features in the electrical conductivity curves by considering both empirical and theoretical evidence. Thus, we will propose an empirical fitting curve, aimed to describe the electrical conductivity of AlCu(Fe,Ru) and AlPdMn samples over the temperature range 4–300 K. We will discuss this proposal on the basis of the spectral conductivity model proposed by Landauro and Solbrig, obtained from *ab initio* band-structure calculations.[68,69] To this end, we derive a closed analytical expression describing the dependence of the electrical conductivity with the temperature. Making use of this expression we will perform a detailed analysis, revisiting the universality of the inverse Matthiessen rule in the light of the obtained results. We also introduce a number of phenomenological coefficients relating the model parameters defining the electronic structure with the fitting coefficients previously obtained.

The paper is organized as follows. In Sec. II we introduce our empirical approach. In Sec. III, we describe the main features of the spectral conductivity model. In Sec. IV, we obtain closed analytical expressions describing the temperature dependence of the electrical conductivity. Section V is devoted to discuss the obtained analytical results in light of pertinent experimental data, highlighting the physical implications of the phenomenological coefficients previously introduced. Finally, we summarize the main conclusions of this work in Sec. VI.

II. EMPIRICAL APPROACH

To motivate our approach in Fig. 1 we compare the temperature dependence of the electrical conductivity for several *i*-QC's belonging to the AlCuFe, AlCuRu, and AlPdMn families. By inspecting this figure several conclusions can

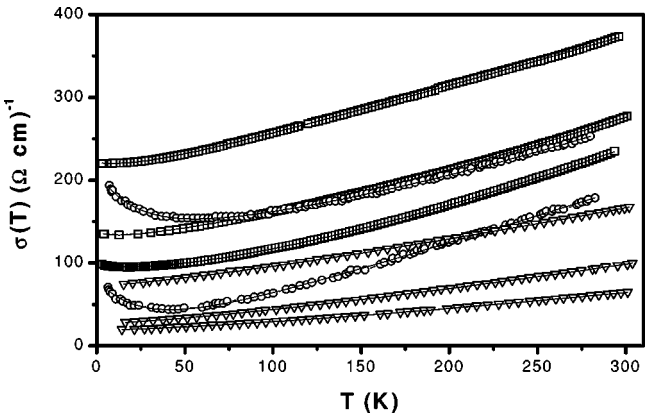

FIG. 1. Electrical conductivity temperature dependencies for different quasicrystalline samples belonging to the AlCuFe (□), AlCuRu (▽), and AlPdMn (○) families. From top to bottom their chemical compositions read as follows: $Al_{63}Cu_{24.5}Fe_{12.5}$, $Al_{62.8}Cu_{24.8}Fe_{12.4}$, $Al_{70}Pd_{20}Mn_{10}$, $Al_{62.5}Cu_{25}Fe_{12.5}$, $Al_{70}Pd_{20}Mn_{10}$, $Al_{65}Cu_{21}Ru_{14}$, $Al_{65}Cu_{20}Ru_{15}$, and $Al_{65}Cu_{19}Ru_{16}$. Solid lines correspond to the best-fit curves listed in Table I. See the main text for details. Data for AlCuFe samples were provided by C. Berger. Data for AlCuRu and AlPdMn samples are after Refs. 30 and 33, respectively.

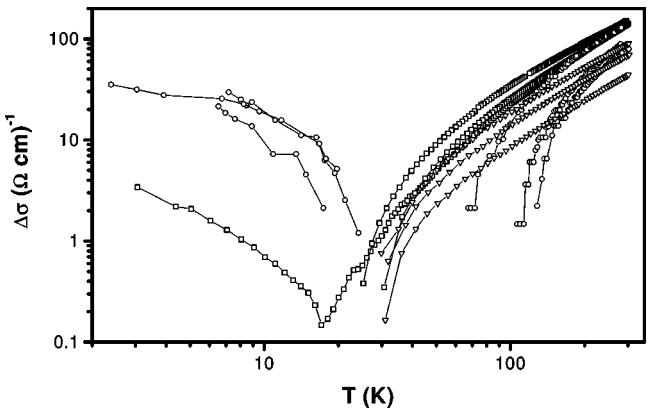

FIG. 2. Log-log diagram comparing the reduced electrical conductivity, $\Delta\sigma(T)=\sigma(T)-\sigma(0)$, temperature dependencies for different quasicrystalline samples belonging to the AlCuFe (□), AlCuRu (▽), and AlPdMn (○) samples shown in Fig. 1. Solid lines are a guide for the eye.

be drawn. First, the presence of a well-defined, broad minimum at about 40–60 K characterizes the $\sigma(T)$ curves of AlPdMn samples. The AlCuFe samples also exhibit a less pronounced minimum at about 10–20 K, depending on the sample stoichiometry. Second, the $\sigma(T)$ curves of AlCuRu samples do not exhibit such a minimum, but monotonously increase over the entire considered temperature range. Third, starting at about 100 K the $\sigma(T)$ curves of both AlCuFe and AlPdMn are markedly parallel to each other (quite remarkably the electrical conductivity curves of the samples $Al_{62.8}Cu_{24.8}Fe_{12.4}$ and $Al_{70}Pd_{20}Mn_{10}$ almost merge). Fourth, although the $\sigma(T)$ curves of the AlCuRu samples are nearly parallel, their common slope is less steep than that corresponding to both AlCuFe and AlPdMn samples. Therefore, attending to their $\sigma(T)$ curves, these quasicrystalline families can be classified into two classes, namely, those exhibiting a well-defined minimum at low temperatures and those which do not exhibit such a minimum.

To further substantiate this scheme, in Fig. 2 the function $\Delta\sigma(T)\equiv\sigma(T)-\sigma(0)$ is shown in a log-log plot for the same samples. Two different behaviors can be clearly appreciated, defining a crossover region located at about $T_c \sim 25$ K. For temperatures above $T\sim 100$ K, the $\Delta\sigma(T)$ curves corresponding to AlCuFe and AlCuRu samples can be described in terms of a power-law function of the form AT^{α}, with different A values but similar values for the exponent. Within this temperature range the AlPdMn samples cannot be described in terms of a power-law function, although such a description becomes progressively adequate at temperatures above $T\sim 200$ K.

On the basis of these empirical results we will start by assuming that the electrical conductivity curve, when considered over a wide temperature range, can be expressed as a sum of two main contributions, namely, $\sigma(T)=\sigma_l(T)+\sigma_h(T)$, where $\sigma_{l,(h)}(T)$ describes the low- (high-) temperature behavior. Accordingly, we propose the following mathematical expression for the temperature dependence of the electrical conductivity curve:

$$\sigma(T)=\sigma_0+A_0e^{-\gamma T}+A_1T^{\alpha}, \tag{2}$$

where σ_0, A_1, and A_0 are measured in $(\Omega\ \mathrm{cm})^{-1}$ units and α and γ take on real values. When $\gamma>0$, the low temperature dependence is mainly determined by the decreasing exponential function, whereas the high-temperature dependence is governed by the power-law function. In this case we have $\sigma_l(T)=\sigma_0+A_0e^{-\gamma T}$ and $\sigma_h(T)=A_1T^{\alpha}$, and a minimum naturally appears when $\sigma_l(T)\simeq\sigma_h(T)$. The residual conductivity in the vanishing temperature limit is given by $\sigma(0)=\sigma_0+A_0$. Here, σ_0 may be related to the possible presence of chemical disorder and/or structural defects, whereas A_0 may be related to the physical process responsible for the upturn of the conductivity at low temperatures, such as the Kondo-like mechanism suggested by Préjean and collaborators.[47] On the other hand, if $\gamma<0$, the resulting growing exponential adds its contribution to the power-law function at any temperature, so that we cannot attain a minimum. In that case $\sigma_l(T)=\sigma_0$, $\sigma_h(T)=A_1T^{\alpha}+A_0e^{-\gamma T}$, and the exponential growth dominates at higher temperatures.

In order to estimate the suitability of Eq. (2) we will fit the data shown in Figs. 1 and 2 to the trial functions listed in Table I. The best-fit curves are plotted in Fig. 1. Fitting analysis results are presented in Tables I and II. From the data listed in these tables several conclusions can be drawn. First, the best possible fit for the AlCuRu samples is obtained for a power-law function ($A_0\equiv 0$), in agreement with the results reported by Lalla and collaborators.[30] Second, Eq. (2) provides the best possible fit for the AlCuFe and AlPdMn samples, although the quality of the fits is considerably better for the former ones. Due to the presence of a broad minimum, neither power-law nor exponential functions alone can fit the $\sigma(T)$ curves corresponding to these samples in the considered temperature range. Hence, Eq. (2) allows for a unified description of the $\sigma(T)$ curves corresponding to dif-

TABLE I. Pearson χ^2 value for different possible fittings to the electrical conductivity curves of the following quasicrystalline samples: (a) $Al_{62.5}Cu_{25}Fe_{12.5}$; (b) $Al_{62.8}Cu_{24.8}Fe_{12.4}$; (c) $Al_{63}Cu_{24.5}Fe_{12.5}$; (d) $Al_{65}Cu_{19}Ru_{16}$; (e) $Al_{65}Cu_{20}Ru_{15}$; (f) $Al_{65}Cu_{21}Ru_{14}$; (g), (h), and (i) $Al_{70}Pd_{20}Mn_{10}$ (under different annealing conditions).

		Sample								
Trial function $\sigma(T)$	Label	a	b	c	d	e	f	g	h	i
$\sigma_0+A_1T^{\alpha}$	I	1.129	0.299	1.349	0.009	0.040	0.091			
$\sigma_0+A_0\ e^{-\gamma T}$	II	5.817	1.435	3.098	0.061	0.222	0.313			
$\sigma_0+A_0\ e^{-\gamma T}+A_1T^{\alpha}$	III	0.053	0.110	0.184				1.864	1.248	1.207
$\sigma(0)(1+BT^2+CT^4+DT^6)$	IV	0.342	0.604	2.168	0.193	0.413	1.139	28.72	51.33	84.94

ferent *i*-QC's over a broad temperature range (4–300 K). Third, the γ parameter corresponding to the trial function II takes negative values. These values are very similar for both AlCuFe and AlCuRu samples (see Table II) yielding a mean value $|\gamma|=0.003\pm0.001$. On the other hand, the γ parameter in the trial function III takes positive values. Their values are very similar for both AlCuFe and AlPdMn samples (see Table II), yielding a mean value $\gamma=0.039\pm0.002$ (we have excluded the value corresponding to the $Al_{62.8}Cu_{24.8}Fe_{12.4}$ sample). If we naively identify $|\gamma|\equiv k_B/\Delta E$, then we, respectively, get $\Delta E_{II}\simeq 29$ meV (trial function II) and $\Delta E_{III}\simeq 2$ meV (trial function III). These figures are too narrow to be interpreted as a measure of a conventional gap, but they compare well with the energy scales corresponding to the dip component of the pseudogap (ΔE_{II}) and to the mean width of the spiky features (ΔE_{III}).

In summary, our fitting analysis suggests that two different temperatures regimes should be considered, each one related to a different transport mechanism. At low temperatures the low diffusivity, determined by the critical nature of electronic states in QC's and/or the presence of different scattering processes, should play a major role. As the temperature is increased, and the energy window k_BT progressively widens, one expects that electronic structure effects should onset, playing an increasingly significant role. In the next section we will focus on this latter physical scenario by considering the influence of band-structure effects in the temperature dependence of the electrical conductivity.

III. ELECTRONIC STRUCTURE MODEL

In this work the study of the transport properties is based on the energy spectrum function $\sigma(E)$, defined as the $T\rightarrow 0$ conductivity with the Fermi level at energy E. Generally speaking the conductivity spectrum takes into account both the DOS structure, $N(E)$, and the diffusivity of the electronic states, $D(E)$, according to the relationship $\sigma(E)\propto N(E)D(E)$. Thus, although it may be tempting to assume that the $\sigma(E)$ function should closely resemble the overall structure of the DOS, it has been shown that a dip in the $\sigma(E)$ curve can correspond to a peak in the DOS at certain energies.[68–70] This behavior is likely to be related to the pe-

TABLE II. Fitting coefficients for different $\sigma(T)$ curves corresponding to the trial functions I–III listed in Table I. AlCuFe data files were provided by C. Berger. Experimental data for AlCuRu and AlPdMn samples were taken from Ref. 30 and Ref. 33, respectively.

Sample	Label	σ_0 $(\Omega\ \mathrm{cm})^{-1}$	A_1 $(\Omega\ \mathrm{cm})^{-1}$	α	A_0 $(\Omega\ \mathrm{cm})^{-1}$	γ (K^{-1})
$Al_{62.5}Cu_{25}Fe_{12.5}$	I	93.2	0.014	1.630	0	
	II	35	-	-	54	−0.005
	III	88	0.029	1.502	10	0.036
$Al_{62.8}Cu_{24.8}Fe_{12.4}$	I	131.7	0.042	1.426	0	
	II	19			107	−0.003
	III	130.4	0.050	1.398	7	0.110
$Al_{63}Cu_{24.5}Fe_{12.5}$	I	215.3	0.155	1.218	0	
	II	−58			270	−0.002
	III	207	0.32	1.099	15	0.042
$Al_{65}Cu_{19}Ru_{16}$	I	18.8	0.019	1.359	0	
	II	−26			43	−0.0025
$Al_{65}Cu_{20}Ru_{15}$	I	26.3	0.045	1.293	0	
	II	−68			92	−0.0020
$Al_{65}Cu_{21}Ru_{14}$	I	72.0	0.078	1.245	0	
	II	−79			149	−0.0017
(g) $Al_{70}Pd_{20}Mn_{10}$	10	0.30	1.12	69	0.039	
(i)$Al_{70}Pd_{20}Mn_{10}$	137	0.02	1.53	72	0.044	
(h) $Al_{70}Pd_{20}Mn_{10}$	31	0.14	1.19	83	0.031	

culiar nature of critical electronic states close to the Fermi level.[64,65,70–72] In fact, recent measurements of photoconductivity in AlPdRe QC's have confirmed the tendency of carriers to localize near the Fermi level.[73]

Regarding the DOS structure, the presence of a pronounced pseudogap at the Fermi level (~1 eV width) was theoretically predicted in order to explain the stability of quasicrystalline alloys on the basis of the Hume-Rothery mechanism.[74] This mechanism has been successfully used to explain the stability of QC's containing elements with a full *d* band, such as AlMgZn or AlCuLi. In the case of QC's bearing transition-metal atoms, such as AlCu(Fe,Ru) or AlPd(Mn,Re), in addition to this broad minimum in the DOS, a narrow dip (~0.1 eV width) due to hybridization effects involving the transition-metal bands should be also taken into account.[75–79] The physical existence of the electronic pseudogap has been confirmed by measurements of the specific-heat capacity,[80] photoemission,[81] soft-x-ray spectroscopies,[82] magnetic susceptibility, and nuclear magnetic-resonance probes.[83] Nevertheless, the relative insensitivity of the specific-heat electronic term to thermal annealing suggests that the presence of the pseudogap alone does not suffice to explain all the transport anomalies, particularly those manifesting themselves at relatively high temperatures, hence implying the influence of band-structure effects.

The possible existence of spiky features in the DOS (over an energy scale of about 10 meV) was obtained from self-consistent *ab initio* calculations,[84] and has been extensively discussed in the literature. The physical origin of such peaks may stem from the structural quasiperiodicity of the substrate via a hierarchical cluster aggregation resonance[56] or through *d*-orbital resonance effects.[85,86] This spiky component is still awaiting a definitive experimental confirmation,[87–91] although recent tunneling spectroscopy measurements provide experimental support for the existence of some fine structure, asymmetrically placed with respect to the Fermi level.[92]

In order to make a meaningful comparison with experimental measurements one should take into account possible phason, finite lifetime, and temperature broadening effects. In so doing, it is observed that most finer details in the DOS are significantly smeared out and only the most conspicuous peaks remain in the vicinity of the Fermi level at room temperature.[2] These considerations convey us to reduce the number of main spectral features necessary to capture the most relevant physics of the transport processes. Two fruitful approaches have been recently considered in the literature to this end. On the one hand, the *ab initio* study performed by Landauro and Solbrig has shown that the spectral resistivity, $\rho(E)$, corresponding to *i*-AlCuFe phases, can be satisfactorily modeled by means of just two basic spectral features, namely, wide and narrow Lorentzian peaks.[68] Quite remarkably, this model is able to properly fit the experimental $\sigma(T)$ and $S(T)$ curves in a broad temperature range.[69] Following a different line of reasoning, aimed to encompass the transport properties of both amorphous phases and QC's within a unified scheme, Häussler and collaborators have shown that the main qualitative features of the $\sigma(T)$, $S(T)$, as well as the Hall coefficient curves can be accounted for by considering

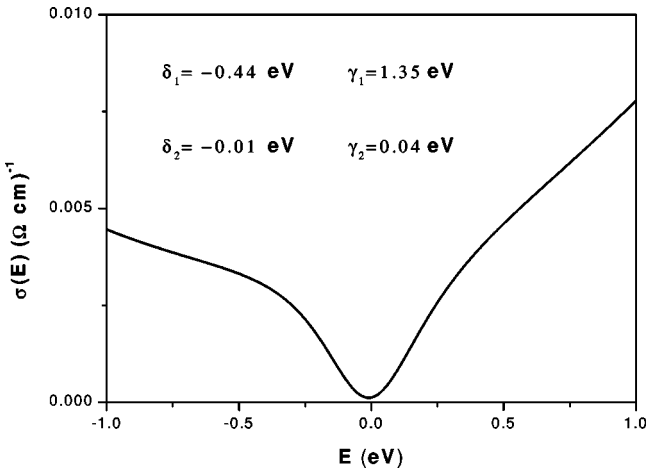

FIG. 3. Spectral conductivity curve in the energy interval ± 1 eV around the Fermi level as obtained from Eq. (3) for the electronic parameter values γ_i and δ_i indicated in the frame.

an *asymmetric* spectral conductivity function characterized by a broad minimum exhibiting a pronounced dip within it.[45]

Motivated by these results, in this work we shall start by considering the following model for the spectral conductivity:[69]

$$\sigma(E) \equiv A[L_1(E)+L_2(E)]^{-1}, \tag{3}$$

where the parameter A is expressed in Ω^{-1} cm^{-1}eV^{-1} units and the Lorentzians

$$L_i(E) = \frac{\gamma_i}{\pi}[\gamma_i^2 + (E-\mu-\delta_i)^2]^{-1} \tag{4}$$

characterize the height, $(\pi\gamma_i)^{-1}$, and position, δ_i, of each spectral feature with reference to the Fermi level, μ. In addition, the γ_i parameters can be related to the diffusivity of the corresponding states.[68,93] For the sake of illustration in Fig. 3 the spectral conductivity curve, as obtained from expression (3), is shown for a suitable choice of the parameters γ_i and δ_i.[68] The overall behavior of this curve agrees well with the experimental results obtained from tunneling and point-contact spectroscopy measurements, where the presence of a dip feature of small width (20–60 meV), superimposed onto a broad (0.5–1 eV), asymmetric pseudogap has been reported.[92,94–97] On the other hand, according to NMR measurements, the DOS within the dip feature energy region can be properly modeled as[65,98]

$$N_d(E) = a + \alpha E^2, \tag{5}$$

where a gives the DOS value at the origin of the energy scale [note that, in general, $a \neq N(\mu)$], and $\alpha \equiv \frac{1}{2}(d^2N/dE^2)$ measures the curvature of the dip. Hence, one expects the conductivity spectrum will exhibit a parabolic dip around the Fermi level. In fact, expanding Eq. (3) in Taylor series around the spectral conductivity minimum, $E_m \equiv 0$, we have

$$\sigma(E) \simeq \sigma_m \left\{ 1 - \frac{\sigma_m}{2A}[L_1''(0)+L_2''(0)]E^2 \right\}, \tag{6}$$

where σ_m is the value of the spectral conductivity at the minimum. By comparing Eqs. (5) and (6), taking into account the Einstein relation $\sigma(E)=e^2N_d(E)D_d(E)$, where e is the electron charge, we get

$$D_d(E)=-\frac{2A\alpha}{e^2a^2[L_1''(0)+L_2''(0)]}, \tag{7}$$

Thus, the diffusivity of the electronic states located in the dip can be approximately estimated from the knowledge of the electronic model parameters and the topology of the $\sigma(E)$ curve. This illustrates the way this approach provides a proper combination of both band-structure effects and the critical nature of the electron wave functions in a natural way.

IV. ANALYTICAL RESULTS AND PHENOMENOLOGICAL COEFFICIENTS

Following previous works[20,26,45,65–69] we will start by expressing the electrical conductivity by

$$\sigma(T)=\int_{-\infty}^{+\infty}dE\left(-\frac{\partial f}{\partial E}\right)\sigma(E), \tag{8}$$

where $f(E,T)$ is the Fermi distribution, and E is the electron energy. In this way we can make use of the knowledge about the energy spectrum obtained from both numerical studies and experimental data, as discussed in the previous section. This treatment is quite general, allowing for a unified treatment of transport properties in QC's. Nevertheless, it should be also stressed that, according to Eq. (8), the effect of the temperature on the transport properties is mainly described by the Fermi distribution temperature dependence. Then, this approach does not take into full account the possible temperature dependence of electron-electron and electron-phonon scattering processes. We should keep in mind this limitation when considering the results discussed in Sec. V.

To proceed we will express Eq. (8) in terms of the scaled variable $x\equiv\beta(E-\mu)$, with $\beta\equiv(k_BT)^{-1}$, to get[65–67]

$$\sigma(T)=\frac{1}{4}\int_{-\infty}^{+\infty}\mathrm{sech}^2(x/2)\sigma(x)dx. \tag{9}$$

Making use of Eq. (3) into Eq. (9) we obtain (see the Appendix)

$$\sigma(\beta)=c_0(\pi^2\beta^{-2}/3+a_3\beta^{-1}H_1/4+a_4H_0/4+a_0), \tag{10}$$

where we have introduced the auxiliary integrals

$$H_k(\beta)\equiv\int_{-\infty}^{\infty}\frac{x^k}{P_2(x)}\mathrm{sech}^2(x/2)dx. \tag{11}$$

In order to evaluate these integrals we shall expand the function $P_2^{-1}(x)$ in Taylor series around the Fermi level to get

$$H_0\simeq\frac{4}{q_0}\left(1+\frac{\pi^2}{3}\frac{4q_1^2-q_0}{q_0^2}\beta^{-2}+\frac{7\pi^4}{15}\frac{q_0^2-12q_0q_1^2+16q_1^4}{q_0^4}\beta^{-4}\right), \tag{12}$$

$$H_1\simeq\frac{8\pi^2q_1\beta^{-1}}{3q_0^2}\left[1+\frac{14\pi^2}{5}\frac{2q_1^2-q_0}{q_0^2}\beta^{-2}+\frac{31\pi^4}{7q_0^4}(4q_1^2-3q_0)(4q_1^2-q_0)\beta^{-4}\right].$$

By plugging Eqs. (12) into (10), keeping $O(\beta^{-6})$ terms,[99] we finally arrive at the following expression for the electrical conductivity:

$$\sigma(T)=c_0\xi_0(1+\xi_2bT^2+\zeta_4b^2T^4+\xi_6b^3T^6), \tag{13}$$

where c_0 is defined in the Appendix, $b\equiv e^2\mathcal{L}_0=2.44\times10^{-8}$ (eV)^2 K^{-2}, $\mathcal{L}_0=\pi^2k_B^2/3e^2=2.44\times10^{-8}$ V^2 K^{-2} is the Lorenz number, and

$$\xi_0\equiv\frac{\gamma_1+\gamma_2}{\varepsilon}, \tag{14}$$

$$\xi_1\equiv-\frac{\gamma_1\delta_1\varepsilon_2^4+\gamma_2\delta_2\varepsilon_1^4}{\varepsilon\varepsilon_1^4\varepsilon_2^4}, \tag{15}$$

$$\xi_2\equiv\frac{\gamma_1\varepsilon_2^6(\varepsilon_1^2-4\delta_1^2)+\gamma_2\varepsilon_1^6(\varepsilon_2^2-4\delta_2^2)}{\varepsilon\varepsilon_1^6\varepsilon_2^6}+4\xi_1^2, \tag{16}$$

$$\zeta_4=\frac{21}{5}\frac{16q_1^2\xi_0^2(\xi_0q_1-\delta_2\varepsilon_1^2)(\xi_0q_1-\delta_1\varepsilon_2^2)+4\varepsilon_2^2\xi_0\varepsilon_1^2\varepsilon_3+\varepsilon_1^4\varepsilon_2^4(\xi_0-\varepsilon_1^2)(\xi_0-\varepsilon_2^2)}{\varepsilon_1^8\varepsilon_2^8}, \tag{17}$$

$$\xi_6\equiv\frac{1116}{7}\frac{\xi_0^2q_1}{\varepsilon_1^{12}\varepsilon_2^{12}}\varepsilon_4(4\xi_0q_1^2-\varepsilon_1^2\varepsilon_2^2)(4\xi_0q_1^2-3\varepsilon_1^2\varepsilon_2^2), \tag{18}$$

where ε is defined in the Appendix, and

$$\varepsilon_3\equiv\xi_0q_1[2\delta_1\varepsilon_2^2+2\delta_2\varepsilon_1^2+q_1(\varepsilon_1^2+\varepsilon_2^2-3\xi_0)]-\varepsilon_1^2\varepsilon_2^2[\delta_1\delta_2+q_1(\delta_1+\delta_2)], \tag{19}$$

$$\varepsilon_4\equiv4\xi_0q_1(q_1-\delta_2)(q_1-\delta_1)+q_1[\xi_0(\varepsilon_1^2+\varepsilon_2^2)-2\varepsilon_1^2\varepsilon_2^2]+\varepsilon_1^2\varepsilon_2^2(\delta_1+\delta_2)-\xi_0(\delta_2\varepsilon_1^2+\delta_1\varepsilon_2^2). \tag{20}$$

The analytically derived ξ_n and ζ_4 coefficients can be regarded as phenomenological parameters containing information about the electronic structure of the sample. In the next section we illustrate the way these phenomenological coefficients can be obtained from a fitting analysis of the experimental $\sigma(T)$ curves.

V. DISCUSSION

In the vanishing temperature limit Eq. (13) reduces to $\sigma(0)=c_0\xi_0$, so that we can rewrite this equation in the closed form[65]

$$\sigma(T)=\sigma(0)[1+e^2\mathcal{L}_0T^2\Lambda(T)], \tag{21}$$

where

$$\Lambda(T)=\xi_2+\zeta_4 bT^2+\xi_6 b^2T^4. \tag{22}$$

Therefore, the electrical conductivity temperature dependence can be separated as a *product* involving two different contributions. The first one is given by the $\sigma(0)$ factor and describes the residual conductivity of the sample. This term will be the one responsible for the overall low-conductivity values observed in these materials and, according to Eq. (14), it can be related to the main features of the spectral conductivity through the relationship

$$\sigma(0)=\pi A\frac{(\gamma_1^2+\delta_1^2)(\gamma_2^2+\delta_2^2)}{\gamma_2(\gamma_1^2+\delta_1^2)+\gamma_1(\gamma_2^2+\delta_2^2)}. \tag{23}$$

This expression provides a direct link between the electronic model parameters γ_i and δ_i and the transport magnitude $\sigma(0)$, which can be determined from the experimental data. The second contribution is given by the function $1+e^2\mathcal{L}_0T^2\Lambda(T)$ and describes the temperature dependence of the electrical conductivity as the temperature is increased. It is worth noting that by identifying $\Delta\sigma(T)\equiv e^2\mathcal{L}_0\sigma(0)T^2\Lambda(T)$, Eq. (21) essentially reduces to the empirically proposed inverse Matthiessen rule given by Eq. (1). Making use of Eq. (23), the $\Delta\sigma(T)$ function can be expressed as

$$\Delta\sigma(T)\equiv U(T)p(T)=(\pi e^2\mathcal{L}_0T^2)\times\left[\frac{A(\gamma_1^2+\delta_1^2)(\gamma_2^2+\delta_2^2)}{\gamma_2(\gamma_1^2+\delta_1^2)+\gamma_1(\gamma_2^2+\delta_2^2)}\Lambda(T)\right]. \tag{24}$$

Therefore, the second term in Eq. (1) can be regarded as a product involving a universal parabolic function, $U(T)\equiv\pi e^2\mathcal{L}_0T^2$, which is modulated by the sample-dependent factor, $p(T)$.[100] The temperature dependence of the $p(T)$ factor is governed by the biquadratic function $\Lambda(T)$, whose coefficients are related to the electronic structure of the sample through the expressions given by Eqs. (15)–(18). To get a clearer picture of the behavior of the $\Lambda(T)$ function we rearrange Eq. (21) to obtain

$$\Lambda(T)=(\sigma(T)-\sigma(0))/(\sigma(0)bT^2). \tag{25}$$

Expressed in this way the $\Lambda(T)$ function can be straightforwardly determined from experimental data. In Fig. 4 the temperature dependence of the $\Lambda(T)$ function is shown in a semilog plot for the same samples shown in Fig. 1. Quite remarkably, at high enough temperatures, the temperature dependence of the $\Lambda(T)$ function apparently exhibits a nearly universal behavior. Note, however, that the $\Lambda(300\ \mathrm{K})$ value varies about an order of magnitude among the considered samples. As it can be clearly appreciated in Fig. 4 the onset of the high-temperature regime depends on the quasicrystalline family we are considering. It starts at temperatures above ~50 K for AlCu(Fe,Ru) samples, and above ~150 K for AlPdMn samples.

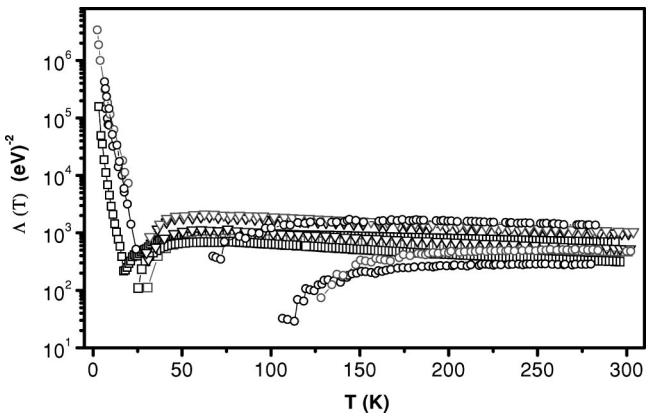

FIG. 4. Diagram comparing the temperature dependencies of the $\Lambda(T)$ function defined by Eq. (22) for different quasicrystalline samples belonging to the AlCuFe (□), AlCuRu (▽), and AlPdMn (○) families listed in Table II. Solid lines are a guide for the eye.

In order to gain some physical understanding on the role played by the different coefficients appearing in Eq. (22) we will fit the experimental $\sigma(T)$ curves shown in Fig. 1 to the trial function

$$\sigma(T)=\sigma(0)(1+BT^2+CT^4+DT^6), \tag{26}$$

where, according to Eq. (13), we have $B\equiv\xi_2 b$, $C\equiv\zeta_4 b^2$, and $D\equiv\xi_6 b^3$. In this way, making use of Eqs. (14)–(18) we can get information about the electronic structure of the different samples from the temperature dependence of the electrical conductivity curves. The fitting analysis results are given in the last entry of Table I (Pearson χ^2) and Table III (fitting coefficients). As a general appreciation, although the χ^2 values corresponding to the trial function IV are not the best possible ones, it is clear that Eq. (13) provides an acceptable alternative fit for both AlCuFe and AlCuRu samples. In addition, by inspecting the data listed in Table III we observe that (i) the B fitting coefficients take very similar values for all the considered samples, (ii) a systematic variation of the C and D fitting coefficients is clearly appreciated, and (iii) the sign of the C and D fitting coefficients corresponding to the AlPdMn sample is reversed with respect to that obtained for the AlCuFe and AlCuRu samples. These trends can also be observed in the related phenomenological coefficients listed in Table IV. In order to gain some physical insight into these coefficients we will take the first and second logarithm derivatives of Eq. (3), obtaining the expressions[101]

TABLE III. Fitting coefficients for different QC $\sigma(T)$ curves corresponding to the trial function labeled IV in Table I.

Sample	$\sigma(0)$ $(\Omega\ \mathrm{cm})^{-1}$	$B\times10^{-5}$ (K^{-2})	$C\times10^{-10}$ (K^{-4})	$D\times10^{-15}$ (K^{-6})
$Al_{62.5}Cu_{25}Fe_{12.5}$	95.0±0.1	2.00±0.02	−1.41±0.05	0.63±0.04
$Al_{62.8}Cu_{24.8}Fe_{12.4}$	136.2±0.2	2.00±0.02	−1.77±0.05	0.96±0.03
$Al_{63}Cu_{24.5}Fe_{12.5}$	226.6±0.3	2.00±0.02	−1.92±0.05	1.08±0.04
$Al_{65}Cu_{21}Ru_{14}$	77.3±0.3	2.00±0.06	−2.5±0.2	1.2±0.1
$Al_{65}Cu_{20}Ru_{16}$	20.6±0.1	5.0±0.1	−3.8±0.3	2.0±0.2
$Al_{65}Cu_{19}Ru_{15}$	29.8±0.2	3.0±0.4	−4.5±0.3	2.3±0.2
$Al_{70}Pd_{20}Mn_{10}$ (g)	49±1	4.0±0.1	+3±1	−3±1

$$\xi_1=\frac{1}{2}\left(\frac{d\ln\sigma(E)}{dE}\right)_{E=\mu}, \tag{27}$$

and

$$\xi_2=\frac{1}{2}\left[\frac{d\ln\sigma(E)}{dE}\right]^2_{E=\mu}+\frac{1}{2}\left[\frac{d^2\ln\sigma(E)}{dE^2}\right]_{E=\mu}. \tag{28}$$

In the temperature ranges we are considering ($4\leqslant T\leqslant 300$ K) the k_BT window spans within the energy region located around the dip feature of the conductivity spectrum ($\sim 0.3-30$ meV), characterized by a positive curvature of the $\sigma(E)$ function (see Fig. 3). Then Eq. (28) implies $\xi_2>0$ in this temperature range. On the other hand, the ξ_1 coefficient can take both positive and negative values, depending on the relative position of the Fermi level with respect to the dip minimum. The magnitude and sign of the phenomenological coefficient ξ_1 can be experimentally determined from the temperature dependence of the Seebeck coefficient in the low-temperature region. In Ref. 101 values within the range $+1.5\lesssim\xi_1\lesssim+8.0\ (\mathrm{eV})^{-1}$ were derived from the $S(T)$ curves of AlCuFe and AlCuRu samples. These figures are consistent with the B values obtained from the above fitting analysis, implying $\xi_2=B/b$ values in the range $+800\lesssim\xi_2\lesssim+2000\ (\mathrm{eV})^{-2}$. Plugging Eq. (27) into Eq. (28) we have

$$\left[\frac{d^2\ln\sigma(E)}{dE^2}\right]_{E=\mu}=2(\xi_2-2\xi_1^2), \tag{29}$$

TABLE IV. Phenomenological coefficients values for several quasicrystalline families as determined from the fitting values listed in Table III.

Sample	ξ_2 $[(\mathrm{eV})^{-2}]$	ζ_4 $[\times10^5(\mathrm{eV})^{-4}]$	ξ_6 $[\times10^7(\mathrm{eV})^{-6}]$
$Al_{62.5}Cu_{25}Fe_{12.5}$	820	−2.37	+4.34
$Al_{62.8}Cu_{24.8}Fe_{12.4}$	820	−2.97	+6.61
$Al_{63}Cu_{24.5}Fe_{12.5}$	820	−3.23	+7.44
$Al_{65}Cu_{21}Ru_{14}$	820	−4.20	+8.26
$Al_{65}Cu_{20}Ru_{16}$	1639	−6.38	+13.77
$Al_{65}Cu_{19}Ru_{15}$	2050	−7.56	+15.83
$Al_{70}Pd_{20}Mn_{10}$ (g)	1230	+5.04	−20.65

so that we can estimate the dip curvature at the Fermi level to be about $\sim 1400\ (\mathrm{eV})^{-2}$. It is interesting to compare this value with that corresponding to the curvature due to the DOS as given by Eq. (5). This value can be determined from the ratio $2\alpha/N(\mu)$. In turn, the value of the second derivative of the DOS at the Fermi level can be estimated from NMR measurements, yielding a $\alpha\simeq 23-32$ state $(\mathrm{eV})^{-3}$/atom for *i*-AlCuRu samples.[102] The DOS value at the Fermi level can be determined from low-temperature specific heat measurements, yielding a $N(\mu)\simeq 0.05$ state $(\mathrm{eV})^{-1}$/atom for *i*-AlCuRu.[19,29] From these figures we get $\alpha/N(\mu)\simeq 450-650\ (\mathrm{eV})^{-2}$. This value compares well with recent DOS curvature estimations, based on a NMR detailed analysis, yielding $\alpha/N(\mu)\simeq 490\ (\mathrm{eV})^{-2}$ for *i*-AlCuFe samples, and $\alpha/N(\mu)\simeq 384\ (\mathrm{eV})^{-2}$ for *i*-AlPdMn samples.[98] This agreement, in turn, suggests that, within the parabolic approximation given by Eq. (6), the second derivative of the diffusivity $D(E)$ plays a subsidiary role as compared to the DOS curvature around the Fermi level.

VI. CONCLUDING REMARKS

We started our study by considering whether the function $\Delta\sigma(T)$ in Eq. (1) can be considered as an universal function describing the temperature dependence of the electrical conductivity for most QC's. According to Eq. (24) we conclude that $\Delta\sigma(T)$ can be expressed as a product involving universal parabolic function, $U(T)\equiv\pi e^2\mathcal{L}_0T^2$, which is modulated by a factor which depends on the electronic structure of the considered sample. This modulation term exhibits a nearly universal behavior at high enough temperatures. The threshold for the onset of the high-temperature regime is sample dependent. In this way, we conclude that the function $\Delta\sigma(T)$ does indeed exhibit certain universal fingerprints, but at the same time plenty of room is left for a significant influence of the electronic structure on the overall behavior of the $\sigma(T)$ curves. Our analytical study allows then to estimate the contribution due to the electronic structure in a precise way by means of Eq. (24).

On the other hand, we have shown that the empirically proposed Eq. (2) provides a unified description of the $\sigma(T)$ curves corresponding to different quasicrystalline families over a broad temperature range. By comparing the $\sigma(T)$ curves given by Eq. (2) and (13) we conclude that the analytically derived $\sigma(T)$ curve is unable to properly describe

the minimum present in both the AlCuFe and AlPdMn families. This shortcoming should then be interpreted as an indication that the very existence of such a minimum cannot be understood in terms of band structure effects alone, but it is necessary to consider other physical processes in the low-temperature regime. To this end, suitable approaches explicitly including the temperature dependence of the spectral conductivity, stemming from scattering processes, should be required. This interpretation is in line with the evidence suggesting a Kondo-like mechanism as the main physical mechanism responsible for the presence of this minimum in AlPdMn samples.[47] In fact, the importance of the fraction of magnetic atoms present in the samples in the transport properties at low temperatures provides additional support for the classification scheme introduced in Sec. II. Thus, although from a chemical viewpoint one may expect that AlCuFe and AlCuRu representatives should be grouped in a similar fashion, our proposed classification, based on their transport properties, splits them into two separate categories. In this sense, the absence of a well-defined minimum for AlCuRu samples may be interpreted as indicating that the *d* states associated with Ru atoms are submerged well below the Fermi level, so that the *sp* electrons dominate the DOS region in the vicinity of E_F, (Ref. 103) (although the possibility of observing a minimum at temperatures below 15 K, not considered in the current experimental data, cannot be excluded either). The existence of some physical trend underlying this twofold classification arises then as a tempting possibility. In this sense, measurements of the electrical conductivities of AlCuOs and AlPdTc icosahedral samples would be very appealing.

Our treatment suggests that the low-conductivity values observed in high quality QC's at low temperatures may stem from two different sources. On the one hand, we have the severe depletion of available charge carriers associated with the presence of a pronounced pseudogap around the Fermi level. On the other hand, we must consider the peculiar nature of critical states, most of which may exhibit quite small group velocities. Although our approach does not allow for a precise estimation of the relative importance of both contributions to the final value of the $\sigma(0)$ term, it represents a promising starting point to future detailed studies.

The phenomenological coefficients introduced in Sec. IV allow us to extract significant information about the electronic structure from experimental $\sigma(T)$ data by means of Eq. (13). The first step is to determine the different ξ_n values from the fitting analysis of the $\sigma(T)$ curve in the way outlined in Sec. V. Then, from the knowledge of the ξ_n, we can determine the electronic model parameters γ_i, δ_i, and A through the analytical expressions derived in Sec. IV. Nonetheless, due to the involved nature of these expressions this is a rather difficult task. Fortunately, even partial knowledge of some of the phenomenological coefficients suffices to gain some physical insight into certain relevant features of the electronic spectrum of the sample, allowing for quantitative estimations about the topology of the spectral conductivity curve, $\sigma(E)$, around the Fermi level. The involved nature of the analytical expressions for the ξ_n coefficients suggests that the study of one transport coefficient alone will not suffice, in general, to get a detailed picture of the sample electronic structure. Therefore, one reasonably expects that a sharper view of the main electronic features of the considered QC samples would ultimately emerge from the simultaneous measurement of different transport coefficients, when analyzed in terms of the framework introduced in this work. In fact, the combined study of the $\sigma(T)$ curve over a broad temperature range and the $S(T)$ curve in the low-temperature limit, mentioned in the previous section, has yielded consistent values for the ξ_1 and ξ_2 coefficients. Thus, our approach provides a *phenomenological* description of the electrical conductivity of QC's, which can contribute to gaining a better understanding of the transport properties in quasicrystalline matter.

In this work we have restricted ourselves to the temperature range from 4 to 300 K, well below the Debye temperature for the considered samples. We have seen that band-structure effects do not to play a significant role in the overall behavior of the $\sigma(T)$ curve at temperatures below, say, 100 K. However, it is reasonable to expect that electronic structure effects would play a more significant role at higher temperatures, where thermally activated processes become important. In this work, we have also focused on the study of Al-transition-metal QC's. Now, since both AlPdMn and AlCu(Fe,Ru) QC's belong to the same structural class, one cannot exclude the possibility that some of the universal features reported may be structure dependent. Consequently, the possible extension of the results discussed in this work to both higher temperatures and other structural types of icosahedral QC's appears as an appealing possibility.

ACKNOWLEDGMENTS

Thanks are warmly due to E. Belin, C. Berger, J. M. Dubois, R. Escudero, T. Grenet, P. Häussler, C. Landauro, D. Mayou, U. Mizutani, S. Roche, and P. A. Thiel for interesting conversations and sharing useful materials. I acknowledge K. Giannò, M. Klanjšek, and A. L. Pope for sharing information and M. V. Hernández for a critical reading of the manuscript. This work was supported by the Consejería de Educación de la CAM and European Union FEDER through Project No. 07N/0070/2001.

APPENDIX

Expressing Eq. (3) in terms of the scaled variable as $\sigma(x)=c_0P_4(x)/P_2(x)$, where

$$P_4(x)\equiv\beta^{-4}x^4-2\beta^{-3}n_3x^3+\beta^{-2}n_2x^2-2\beta^{-1}n_1x+n_0,$$

$$P_2(x)\equiv\beta^{-2}x^2-2\beta^{-1}q_1x+q_0,$$

where $c_0\equiv\pi A(\gamma_1+\gamma_2)^{-1}$, $n_3\equiv\delta_1+\delta_2$, $n_2\equiv\varepsilon_1^2+\varepsilon_2^2+4\delta_1\delta_2$, $n_1\equiv\delta_2\varepsilon_1^2+\delta_1\varepsilon_2^2$, $n_0\equiv\varepsilon_1^2\varepsilon_2^2$, $q_0\equiv\varepsilon\varepsilon_1^2\varepsilon_2^2(\gamma_1+\gamma_2)^{-1}$, and $q_1=(\gamma_1\delta_2+\delta_1\gamma_2)(\gamma_1+\gamma_2)^{-1}$, with $\varepsilon_i^2\equiv\gamma_i^2+\delta_i^2$, and $\varepsilon\equiv\gamma_1\varepsilon_1^{-2}+\gamma_2\varepsilon_2^{-2}$, we can rewrite Eq. (8) in the form

$$\sigma(\beta)=\frac{c_0}{4}\int_{-\infty}^{\infty}\left[\sum_{k=0}^{2}a_k\beta^{-k}x^k+\frac{a_3\beta^{-1}x+a_4}{P_2(x)}\right]\times\operatorname{sech}^2(x/2)dx,$$

where

$$a_0\equiv 2a_1q_1+n_2-q_0=\frac{(\gamma_1+\gamma_2)(\gamma_1\varepsilon_1^2+\gamma_2\varepsilon_2^2)-4\gamma_1\gamma_2\Delta\delta^2}{(\gamma_1+\gamma_2)^2},$$

$$a_1\equiv 2(q_1-n_3)=-2\frac{\delta_1\gamma_1+\delta_2\gamma_2}{\gamma_1+\gamma_2},\quad a_2=1,$$

$$a_3\equiv 2a_0q_1-2n_1-a_1q_0=-4\gamma_1\gamma_2\Delta\delta\frac{2q_1\Delta\delta-\varepsilon_1^2+\varepsilon_2^2}{(\gamma_1+\gamma_2)^2},$$

$$a_4\equiv n_0-a_0q_0=\gamma_1\gamma_2\frac{4\varepsilon\varepsilon_1^2\varepsilon_2^2\Delta\delta^2-(\varepsilon_1^2-\varepsilon_2^2)^2(\gamma_1+\gamma_2)}{(\gamma_1+\gamma_2)^3},$$

with $\Delta\delta\equiv\delta_1-\delta_2$. Making use of the integrals

$$\int_{-\infty}^{\infty}\operatorname{sech}^2(x/2)dx=4,\quad\int_{-\infty}^{\infty}x^2\operatorname{sech}^2(x/2)dx=\frac{4\pi^2}{3},$$

$$\int_{-\infty}^{\infty}x^4\operatorname{sech}^2(x/2)dx=\frac{28\pi^4}{15},$$

$$\int_{-\infty}^{\infty}x^6\operatorname{sech}^2(x/2)dx=\frac{124\pi^6}{21},$$

and

$$\int_{-\infty}^{\infty}x^l\operatorname{sech}^2(x/2)dx=0,\quad (l\text{odd}),$$

we then obtain Eq. (10).

[1] A.P. Tsai, in *Physical Properties of Quasicrystals*, edited by Z.M. Stadnik, Springer Series in Solid-State Physics, Vol. 126 (Springer-Verlag, Berlin, 1999), p. 5.

[2] Z.M. Stadnik, D. Purdie, Y. Baer, and T.A. Lograsso, Phys. Rev. B **64**, 214202 (2001); Z.M. Stadnik, in *Physical Properties of Quasicrystals* (Ref. 1), p. 257.

[3] E. Maciá, J.M. Dubois, and P.A. Thiel, *Ullmann's Encyclopedia of Industrial Chemistry*, 6th ed., 2002 January release on CD-ROM (Wiley-VCH, Weinheim, 2002).

[4] Ö. Rapp, in *Physical Properties of Quasicrystals* (Ref. 1), p. 127.

[5] S. Roche, G. Trambly de Laissardière, and D. Mayou, J. Math. Phys. **38**, 1794 (1997).

[6] S. Legault, B. Ellman, J.O. Ström-Olsen, L. Taillefer, S. Kycia, T. Lograsso, and D. Delaney, in *New Horizons in Quasicrystals: Research and Applications*, edited by A.I. Goldman, D.J. Sordelet, P.A. Thiel, and J.M. Dubois (World Scientific, Singapore, 1997), p. 224.

[7] M.A. Chernikov, A. Bianchi, and H.R. Ott, Phys. Rev. B **51**, 153 (1995); P.A. Kalugin, M.A. Chernikov, A. Bianchi, and H.R. Ott, *ibid.* **53**, 14 145 (1996); M.A. Chernikov, E. Felder, A. Bianchi, C. Wälti, M. Kenzelmann, H.R. Ott, K. Edagawa, M. de Boissieu, C. Janot, M. Feuerbacher, N. Tamura, and K. Urban, in *Proceedings of the 6th International Conference on Quasicrystals*, edited by S. Takeuchi and T. Fujiwara (World Scientific, Singapore, 1998), p. 451.

[8] C. Berger, in *Lectures on Quasicrystals*, edited by F. Hippert and D. Gratias (Les Editions de Physique, Les Ulis, 1994).

[9] J.S. Poon, Adv. Phys. **41**, 303 (1992).

[10] K. Kirihara and K. Kimura, Science and Technology of Advanced Materials **1**, 227 (2000); R. Tamura, A. Waseda, K. Kimura, and H. Ino, Phys. Rev. B **50**, 9640 (1994).

[11] T. Klein, C. Berger, D. Mayou, and F. Cyrot-Lackmann, Phys. Rev. Lett. **66**, 2907 (1991).

[12] A. Carlsson, Nature (London) **353**, 353 (1991).

[13] F.S. Pierce, Q. Quo, and J. Poon, Phys. Rev. Lett. **73**, 2220 (1994).

[14] T. Klein and O.G. Symko, Phys. Rev. Lett. **73**, 2248 (1994).

[15] E. Maciá, Appl. Phys. Lett. **81**, 88 (2002).

[16] K. Kimura, H. Iwahashi, T. Hashimoto, S. Takeuchi, U. Mizutani, S. Ohashi, and G. Itoh, J. Phys. Soc. Jpn. **58**, 2472 (1989).

[17] U. Mizutani, Y. Sakabe, T. Shibuya, K. Kimura, and S. Takeuchi, J. Phys.: Condens. Matter **2**, 6169 (1990).

[18] J.L. Wagner, B.D. Biggs, and S.J. Poon, Phys. Rev. Lett. **65**, 203 (1990).

[19] B.D. Biggs, S.J. Poon, and N.R. Munirathnam, Phys. Rev. Lett. **65**, 2700 (1990).

[20] F.S. Pierce, S.J. Poon, and B.D. Biggs, Phys. Rev. Lett. **70**, 3919 (1993).

[21] F.S. Pierce, S.J. Poon, and Q. Guo, Science **261**, 737 (1993).

[22] B.D. Biggs, Y. Li, and S.J. Poon, Phys. Rev. B **43**, 8747 (1991).

[23] T. Klein, C. Berger, D. Mayou, and F. Cyrot-Lackmann, Phys. Rev. Lett. **66**, 2907 (1991).

[24] T. Klein, A. Gozlan, C. Berger, F. Cyrot-Lackmann, Y. Calvaryac, and A. Quivy, Europhys. Lett. **13**, 129 (1990).

[25] T. Klein, H. Rakoto, C. Berger, G. Fourcaudot, and F. Cyrot-Lackmann, Phys. Rev. B **45**, 2046 (1992).

[26] F.S. Pierce, P.A. Bancel, B.D. Biggs, Q. Guo, and S.J. Poon, Phys. Rev. B **47**, 5670 (1993).

[27] R. Haberken, G. Fritsch, and M. Härting, Appl. Phys. A: Mater. Sci. Process. **57**, 431 (1993).

[28] M.A. Chernikov, A. Bernasconi, C. Beeli, and H.R. Ott, Europhys. Lett. **21**, 767 (1993).

[29] F.S. Pierce, Q. Guo, and S.J. Poon, Phys. Rev. Lett. **73**, 2220 (1994).

[30] N.P. Lalla, R.S. Tiwari, and O.N. Srivastava, J. Phys.: Condens. Matter **7**, 2409 (1995).

[31] C. Cignoux, C. Berger, G. Fourcaudot, J.C. Grieco, and H. Rakoto, Europhys. Lett. **39**, 171 (1997).

[32] F. Giraud, T. Grenet, C. Berger, P. Lindqvist, C. Gignoux, and G.

Fourcaudot, Czech. J. Phys. **46**, 2709 (1996).
[33] T.M. Tritt, A.L. Pope, M. Chernikov, M. Feuerbacher, S. Legault, R. Cagnon, and J. Strom-Olsen, Mater. Res. Soc. Symp. Proc. No. 553, (Materials Research Society, Pittsburgh, 1999), p. 489; A.L. Pope, T.M. Tritt, M. Chernikov, M. Feuerbacher, S. Legault, R. Cagnon, and J. Strom-Olsen, *ibid.* **545**, 413 (1999).
[34] A. Bilušic, D. Pavuna, and A. Smontara, Vacuum **61**, 345 (2001); A. Bilušic, A. Smontara, J.C. Lasjaunias, J. Ivkov, and Y. Calvayrac, Mater. Sci. Eng., A **294-296**, 711 (2000).
[35] A.L. Pope, T.M. Tritt, M.A. Chernikov, and M. Feuerbacher, Appl. Phys. Lett. **75**, 1854 (1999); A.L. Pope, R. Schneidmiller, J.W. Kolis, T.M. Tritt, R. Gagnon, J. Strom-Olsen, and S. Legault, Phys. Rev. B **63**, 052202 (2001).
[36] V. Fournée, U. Mizutani, T. Takeuchi, K. Saitoh, M. Ikeyama, J.Q. Guo, and A.P. Tsai, Mater. Res. Soc. Symp. Proc. No. 643 (Materials Research Society, Pittsburgh, 2001), K14.3.1.
[37] K. Giannò, A.V. Sologubenko, L. Liechtenstein, M.A. Chernikov, and H.R. Ott, Ferroelectrics **250**, 249 (2001).
[38] R. Haberken, K. Khedhri, C. Madel, and P. Häussler, Mater. Sci. Eng., A **294-296**, 475 (2000).
[39] K. Kirihara, T. Nagata, and K. Kimura, J. Alloys Compd. **342**, 469 (2002).
[40] K. Giannò, A.V. Sologubenko, M.A. Chernikov, H.R. Ott, I.R. Fisher, and P.C. Canfield, Mater. Sci. Eng., A **294-296**, 715 (2000).
[41] A.L. Pope, T.M. Tritt, R. Gagnon, and J. Strom-Olsen, Appl. Phys. Lett. **79**, 2345 (2001).
[42] D. Mayou, C. Berger, F. Cyrot-Lackmann, T. Klein, and P. Lanco, Phys. Rev. Lett. **70**, 3915 (1993).
[43] In their original work the decomposition involves the experimentally measured quantity $\sigma(4\ \mathrm{K})$ instead of the extrapolated value $\sigma(0)$. In some instances this extrapolation may be unclear because the conductivity curve exhibits succesive curvature changes as the zero-temperature limit is attained. This is the case for AlPdRe at ultralow temperatures, as discussed in Ref. 48.
[44] A. Quivy, M. Quiquandon, Y. Calvaryac, F. Faudot, D. Gratias, C. Berger, R.A. Brand, V. Simonet, and F. Hippert, J. Phys.: Condens. Matter **8**, 4223 (1996).
[45] P. Häussler, R. Haberken, C. Madel, J. Barzola-Quiquia, and M. Lang, J. Alloys Compd. **342**, 228 (2002); P. Häussler, H. Nowak, and R. Haberken, Mater. Sci. Eng., A **294-296**, 283 (2000); C. Roth, G. Schwalbe, R. Knöfler, F. Zavaliche, O. Madel, R. Haberkern, and P. Häussler, J. Non-Cryst. Solids **252**, 869 (1999).
[46] In this work we do not consider QC's bearing rare-earth elements.
[47] J.J. Préjean, C. Berger, A. Sulpice, and Y. Calvaryac, Phys. Rev. B **65**, 140203 (2002).
[48] J. Delahaye and C. Berger, Phys. Rev. B **64**, 094203 (2001); J. Delahaye, C. Berger, T. Grenet, and G. Fourcaudot, Mater. Res. Soc. Symp. Proc. No. 643 (Materials Research Society, Pittsburgh, 2001), K13.2.
[49] A.F. Prekul, N.Yu. Kuzmin, and N.J. Shchegolikhina, Mater. Sci. Eng., A **294-296**, 527 (2000).
[50] M. Rodmar, M. Ahlgren, D. Oberschmidt, C. Gignoux, J. Delahaye, C. Berger, S.J. Poon, and Ö. Rapp, Phys. Rev. B **61**, 3936 (2000); Ö. Rapp, Mater. Sci. Eng., A **294-296**, 458 (2000).
[51] T. Grenet and F. Giroud, Eur. Phys. J. B **23**, 165 (2001).
[52] M. Goda and H. Kubo, J. Phys. Soc. Jpn. **58**, 2109 (1989).
[53] C. Sire, in *Lectures on Quasicrystals* (Ref. 8).
[54] T. Fujiwara, in *Physical Properties of Quasicrystals* (Ref. 1), p. 169.
[55] J. Bellissard, Mater. Sci. Eng., A **294-296**, 450 (2000).
[56] C. Janot and M. de Boissieu, Phys. Rev. Lett. **72**, 1674 (1994); C. Janot, Phys. Rev. B **53**, 181 (1996).
[57] S.E. Burkov, A.A. Varlamov, and D.V. Livanov, Phys. Rev. B **53**, 11 504 (1996).
[58] Yu.Kh. Vekilov and E.I. Isaev, Ferroelectrics **250**, 343 (2001).
[59] N. Rivier and M. Durand, Mater. Sci. Eng., A **294-296**, 584 (2000).
[60] Yu.Kh. Vekilov, E.I. Isaev, and S.F. Arslanov, Ferroelectrics **250**, 339 (2001); P.A. Kalugin, A.Yu. Kitaev, and L.S. Levitov, Zh. Éksp. Teor. Fiz **91**, 692 (1986) [Sov. Phys. JETP **64**, 410 (1986)].
[61] B. Passuro, C. Sire, and V.G. Benza, Phys. Rev. B **46**, 13 751 (1992).
[62] H. Solbrig and C.V. Landauro, Adv. Solid State Phys. **42**, 151 (2002).
[63] E. Maciá, F. Domínguez-Adame, and A. Sánchez, Phys. Rev. B **49**, 9503 (1994).
[64] E. Maciá and F. Domínguez-Adame, *Electrons, Phonons, and Excitons in Low Dimensional Aperiodic Systems* (Editorial Complutense, Madrid, 2000).
[65] E. Maciá, Phys. Rev. B **61**, 8771 (2000).
[66] E. Maciá, Appl. Phys. Lett. **77**, 3045 (2000).
[67] E. Maciá, Phys. Rev. B **64**, 094206 (2001).
[68] C.V. Landauro and H. Solbrig, Mater. Sci. Eng., A **294-296**, 600 (2000).
[69] C.V. Landauro and H. Solbrig, Physica B **301**, 267 (2001).
[70] S. Roche and D. Mayou, Phys. Rev. Lett. **79**, 2518 (1997).
[71] P.A. Thiel and J.M. Dubois, Nature (London) **406**, 570 (2000).
[72] E. Maciá and F. Domínguez-Adame, Phys. Rev. Lett. **76**, 2957 (1996); E. Maciá, Phys. Rev. B **60**, 10 032 (1999).
[73] M. Takeda, R. Tamura, Y. Sakairi, and K. Kimura, in *Proceedings of the 6th International Conference on Quasicrystals*, edited by S. Takeuchi and T. Fujiwara (World Scientific, Singapore, 1998), p. 571; Y. Sakairi, M. Takeda, R. Tamura, K. Edagawa, and K. Kimura, Mater. Sci. Eng., A **294-296**, 519 (2000).
[74] J. Friedel, Helv. Phys. Acta **61**, 538 (1988); T. Fujiwara and T. Yokokawa, Phys. Rev. Lett. **66**, 333 (1991).
[75] G. Trambly de Laissardière, D. Mayou, and D. Nguyen Manh, Europhys. Lett. **21**, 25 (1993).
[76] G. Trambly de Laissardière, D. Nguyen Manh, L. Magaud, J.P. Julien, F. Cyrot-Lackmann, and D. Mayou, Phys. Rev. B **52**, 7920 (1995).
[77] U. Mizutani, Mater. Trans., JIM **42**, 901 (2001); U. Mizutani, T. Takeuchi, E. Banno, V. Fourneé, M. Takata, and H. Sato, Mater. Res. Soc. Symp. Proc. No. 643 (Materials Research Society, Pittsburgh, 2001), K13.1.1.
[78] M. Krajčí and J. Hafner, J. Phys.: Condens. Matter **14**, 1865 (2002).
[79] V. Fournee, E. Belin-Ferre, P. Pecheur, J. Tobola, Z. Dankhazi, A. Sadoc, and H. Müller, J. Phys.: Condens. Matter **14**, 87 (2002).
[80] T. Klein, C. Berger, D. Mayou, and F. Cyrot-Lackmann, Phys. Rev. Lett. **66**, 2907 (1991); F.S. Pierce, P.A. Bancel, D.B. Biggs, Q. Guo, and S.J. Poon, Phys. Rev. B **47**, 5670 (1993); M.A. Chernikov, A. Bianchi, E. Felder, U. Gubler, and H.R. Ott, Europhys. Lett. **35**, 431 (1996).
[81] M. Mori, S. Matsuo, T. Ishimasa, T. Matsuura, K. Kamiya, H.

Inokuchi, and T. Matsukawa, J. Phys.: Condens. Matter **3**, 767 (1991).
[82] E. Belin, Z. Dankhazi, A. Sadoc, Y. Calvayrac, T. Klein, and J.M. Dubois, J. Phys.: Condens. Matter **4**, 4459 (1992).
[83] A. Shastri, F. Borsa, A.I. Goldman, J.E. Shield, and D.R. Torgeson, J. Non-Cryst. Solids **153&154**, 347 (1993); Phys. Rev. B **50**, 15 651 (1994); Z.M. Stadnik, in *Physical Properties of Quasicrystals* (Ref. 1).
[84] T. Fujiwara, S. Yamamoto, and G. Trambly de Laissardière, Phys. Rev. Lett. **71**, 4166 (1993); G. Trambly de Laissardière and T. Fujiwara, Phys. Rev. B **50**, 5999 (1994); G. Trambly de Laissardière and T. Fujiwara, *ibid.* **50**, 9843 (1994).
[85] G. Trambly de Laissardière and D. Mayou, Phys. Rev. B **55**, 2890 (1997); G. Trambly de Laissardière, S. Roche and D. Mayou, Mater. Sci. Eng., A **226-228**, 986 (1997).
[86] H. Solbrig and C.V. Landauro, Physica B **292**, 47 (2000).
[87] Z.M. Stadnik and G. Stroink, Phys. Rev. B **47**, 100 (1993); G.W. Zhang, Z.M. Stadnik, A.-P. Tsai, and A. Inoue, *ibid.* **50**, 6696 (1994); A. Shastri, D.B. Baker, M.S. Conradi, F. Borsa, and D.R. Torgeson, *ibid.* **52**, 12 681 (1995).
[88] Z.M. Stadnik, D. Purdie, M. Garnier, Y. Baer, A.-P. Tsai, A. Inoue, K. Edagawa, and S. Takeuchi, Phys. Rev. Lett. **77**, 1777 (1996); Z.M. Stadnik, D. Purdie, M. Garnier, Y. Baer, A.-P. Tsai, A. Inoue, K. Edagawa, S. Takeuchi, and K.H.J. Buschow, Phys. Rev. B **55**, 10 938 (1997)
[89] P. Lindqvist, P. Lanco, C. Berger, A.G.M. Jansen, and F. Cyrot-Lackmann, Phys. Rev. B **51**, 4796 (1995).
[90] Ph. Ebert, M. Feuerbacher, N. Tamura, M. Wollgarten, and K. Urban, Phys. Rev. Lett. **77**, 3827 (1996).
[91] T. Schaub, J. Delahaye, C. Berger, H. Guyot, R. Belkhou, A. Taleb-Ibrahimi, and Y. Calvayrac, Eur. Phys. J. B **20**, 183 (2001).
[92] R. Escudero, J.C. Lasjaunias, Y. Calvayrac, and M. Boudard, J. Phys.: Condens. Matter **11**, 383 (1999).
[93] S. Roche and T. Fujiwara, Phys. Rev. B **58**, 11 338 (1998).
[94] T. Klein, O.G. Symko, D.N. Davydov, and A.G.M. Jansen, Phys. Rev. Lett. **74**, 3656 (1995).
[95] D.N. Davydov, D. Mayou, C. Berger, C. Gignoux, A. Neumann, A.G.M. Jansen, and P. Wyder, Phys. Rev. Lett. **77**, 3173 (1996).
[96] X.P. Tang, E.A. Hill, S.K. Wonnell, S.J. Poon, and Y. Wu, Phys. Rev. Lett. **79**, 1070 (1997).
[97] T. Klein, O.G. Symko, D.N. Davydov, and A.G.M. Jansen, Phys. Rev. Lett. **74**, 3656 (1995); D.N. Davydov, D. Mayou, C. Berger, C. Gignoux, A. Neumann, A.G.M. Jansen, and P. Wyder, *ibid.* **77**, 3173 (1996).
[98] J. Dolinšek, M. Klanjšek, T. Apih, A. Smontara, J.C. Lasjaunias, J.M. Dubois, and S.J. Poon, Phys. Rev. B **62**, 8862 (2000).
[99] We have verified that if we truncate the expansion series including up to $O(\beta^{-3})$ terms only, the resulting expressions for $\sigma(T)$ cannot be satisfactorily fitted to the experimental data beyond $T \simeq 300$ K.
[100] The parabolic factor $U(T)$ can also be obtained from the Sommerfeld expansion of Eq. (8). See, for example, H. Solbrig and C.V. Landauro, Ref. 62.
[101] E. Maciá, J. Appl. Phys. (to be published).
[102] C.A. Hill, T.C. Chang, Y. Wu, S.J. Poon, F.S. Pierce, and Z.M. Stadnik, Phys. Rev. B **49**, 8615 (1994).
[103] U. Mizutani, Y. Sakabe, T. Shibuya, K. Kishi, K. Kimura, and S. Takeuchi, J. Phys.: Condens. Matter **2**, 6169 (1990).